

Ligand-Induced Conformational Changes in Lactose Repressor: A Fluorescence Study of Single Tryptophan Mutants[†]

Jennifer K. Barry and Kathleen S. Matthews*

Department of Biochemistry and Cell Biology, Rice University, Houston, Texas 77005-1892

Received July 11, 1997; Revised Manuscript Received September 17, 1997[®]

ABSTRACT: A key element in the ability of *lac* repressor protein to control transcription reversibly is the capacity to assume different conformations in response to ligand binding. To investigate regions of the protein involved in these conformational changes, mutant repressor proteins containing single tryptophans were created by mutating each of the two native tryptophan residues to tyrosine and changing the residue of interest to tryptophan. Tryptophans substituted in the following locations were highly accessible to quenchers with no changes in fluorescence or quenching properties in the presence of ligands: in the N-terminal helix–turn–helix for Y7, at the junction between the N-terminus and N-subdomain for L62, in the N-subdomain of the monomer–monomer interface for residue E100 or Q117, or at the C-terminal region for K325. Tryptophan at position F226 in the C-subdomain subunit interface was only moderately exposed to quenchers and unresponsive to ligands. In contrast, the fluorescence and quenching properties of single tryptophans placed in the central region of the protein were affected by ligands. Inducer binding altered the accessibility to quencher for tryptophan at H74 or F293, but no changes were detected upon binding operator. Exposure of tryptophan at the position occupied by Y273 was affected by both inducer and operator, indicating alterations in this region by both ligands. These results suggest that, in the areas of the *lac* repressor probed by these substitutions, the inducer-bound form differs from the conformation of the unliganded form.

The *lac* repressor protein regulates the expression of the genes for lactose metabolism in *Escherichia coli* by high-affinity association with the *lac* operator sequence (1). The *lac* repressor protein is a 150 000 kDa homotetramer (2, 3) which associates through two different subunit interfaces, monomer–monomer and dimer–dimer. The distinction between these interfaces was derived originally from physical and genetic studies (4–8) and confirmed by recent X-ray crystallographic structures (9, 10). The structural elements involved in assembly to tetramer are located in the core domain (amino acids 60–360) which binds the inducing sugars (9–14). The monomer–monomer interface is stabilized by hydrophobic and polar interactions distributed within the core region (9, 10, 14–17), and the dimer–dimer interface is formed by a leucine heptad repeat sequence at the extreme C-terminus (amino acids 342–356) (4–7, 9, 10). The N-terminus of the protein (amino acids 1–59) creates the operator binding site when two N-termini are correctly positioned relative to each other in the dimer structure (10, 18–21).

Inducer binding to *lac* repressor reduces its affinity for operator DNA to that of nonspecific DNA, apparently via a conformational change along the monomer–monomer interface (1, 2, 10, 22–26). Conversely, the affinity of operator-bound protein for inducer is decreased 10-fold (27, 28). These reciprocal changes in ligand affinity suggest that *lac* repressor can exist in at least two discrete conforma-

tions: operator-bound or inducer-bound. In addition, the unliganded conformation may differ from either of the bound forms. The structure of each of these conformations has been solved by X-ray crystallography (10). In the operator-bound structure, there are structural rearrangements which occur in comparison to the other two crystallographic structures. The changes in response to operator complex formation appear to be a rearrangement of how the monomers are oriented in the monomer–monomer interface. Similar changes in conformation were detected in the orientation of the free versus the operator-bound holoprotein in the crystal structures of purine repressor, a member of the *LacI* family with homology to *lac* repressor (29, 30). Although the crystallographic structures suggest that the unliganded and inducer-bound conformations of *lac* repressor are similar, there is a significant body of evidence for conformational differences between unliganded and inducer-bound repressor. These studies include effects of inducer on reactivity or spectroscopic properties of side chains dispersed throughout the sequence and on physical properties of the protein (31–43). Therefore, the similarity of the free and inducer-bound crystallographic structures conflicts with previous biochemical and biophysical data.

The crystallographic structures of *lac* repressor bound to different ligands may provide information about the final conformations that the protein can assume upon ligand binding. However, the dynamic processes and possible intermediate structures involved in the transitions between conformations are not evident from these structures. A full understanding of ligand binding and conformational changes occurring in *lac* repressor requires analysis of these events in solution under controlled reaction conditions. Such conformational changes in proteins can be monitored using

[†] Support for this project was provided by grants to K.S.M. from the NIH (GM 22441) and the Robert A. Welch Foundation (C-576). Spectroscopic facilities utilized were provided by the Keck Center for Computational Biology and the Lucille P. Markey Charitable Trust.

* To whom correspondence should be addressed: phone, 713-527-4871; fax, 713-285-5154; email, ksm@bioc.rice.edu.

[®] Abstract published in *Advance ACS Abstracts*, November 15, 1997.

tryptophan fluorescence emission. Some proteins contain intrinsic tryptophans conveniently located for these measurements. However, in some cases, the tryptophan residues are too far removed from the region of interest, or the relevant fluorescence signal is lost in the background from other tryptophan residues. Site-directed mutagenesis has aided studies of specific tryptophan residues by allowing removal of native tryptophans and placement of single tryptophans in areas of interest. Single tryptophan-containing proteins have been used to monitor conformational changes or ligand binding in many proteins, including *lac* repressor, galactose repressor, *lac* permease, fructose 6-phosphate, 2-kinase: fructose 2,6-bisphosphatase, yeast 3-phosphoglycerate kinase, and recA protein (40, 42, 44–48).

The two native tryptophans in *lac* repressor (residues 201 and 220) have been converted to tyrosine and characterized individually (40, 42). However, the native tryptophans in *lac* repressor are located in the inner apolar region of the C-terminal domain and inducer binding pocket of the protein, respectively, and other areas that may be affected by ligand binding could not be monitored. In the present study, a “tryptophan-less” (Wless)¹ *lac* repressor was produced to remove the native fluorescence emission of W201 and W220, and single tryptophans were introduced at multiple sites, including the DNA binding region, the monomer–monomer subunit interface, and the inducer binding pocket. These areas are predicted to undergo conformational changes during ligand binding. The regions selected for substitution were identified on the basis of a model of the *lac* repressor monomer, the purine repressor crystallographic structure, and the structures of the *lac* repressor core and intact ligand-bound species (9, 10, 29, 30, 49). Previously published phenotypic screens of numerous *lac* repressor mutants were used to discern which amino acids within these regions might be mutated to tryptophan with minimal disruption to protein function (14). Steady-state, quenching, and time-resolved fluorescence properties of the single tryptophan mutant proteins were measured to monitor the effects of inducer and operator binding.

MATERIALS AND METHODS

Mutagenesis. Mutations in the *lac* repressor gene were generated in the pAC1 plasmid (16) using the method of Kunkel (50). The pAC1 plasmid containing the *lac* repressor gene with the W220Y mutation (42) was used to produce the W201Y/W220Y double mutant. All single tryptophan repressors were produced by annealing an oligonucleotide containing the mutant sequence to the uracil-containing template with the W201Y/W220Y mutation. The annealing mixture was heated at 75 °C for 2 min and then allowed to cool to room temperature. The extension and ligation reactions were carried out as described in Li and Matthews (51).

Purification. Protein purification followed the previously described procedure (6), with the following changes to the phosphocellulose column protocol. The dialyzed fraction containing the *lac* repressor protein was spun at 27200g for 30 min to remove any precipitate before being loaded onto

a phosphocellulose column equilibrated in 0.08 M potassium phosphate, pH 7.5. The column was washed with the same buffer, followed by 0.12 M potassium phosphate buffer wash, and protein was eluted with a gradient from 0.12 to 0.3 M potassium phosphate. Protein concentrations for mutants were determined by Bradford assay (52) using wild-type *lac* repressor as a standard.

Operator Binding. Operator binding constants were determined for the proteins using the nitrocellulose filter binding assay (23) modified for use in a 96-well dot blot apparatus (53). The assay was carried out at room temperature in FB buffer (0.01 M Tris-HCl, pH 7.4, 0.15 M KCl, 0.1 mM DTT, 0.1 mM EDTA, and 5% DMSO) with 100 µg/mL bovine serum albumin. The operator used was a 40 base pair double-stranded DNA (sequence: 5'-TGTTGTGTGGAATTGTGAGCGGATAACAATTTTCACACAGG-3') which was labeled at the 5' end with ³²P by polynucleotide kinase reaction. The concentration of labeled operator in the assay was $\sim 5 \times 10^{-12}$ M (27). The concentration of protein was varied from 2.5×10^{-12} to 1.25×10^{-9} M tetramer. The amount of ³²P-operator bound at each protein concentration was quantified as pixels by a Fuji phosphorimager. All data were normalized by dividing the pixels at the different protein concentrations by the pixels at a saturating concentration. These data were fitted to the equation:

$$R = [P]/(K_d + [P]) \quad (1)$$

where R is the relative fraction of bound complexes within each solution calculated by $R = \text{operator bound}/\text{operator bound}_{\text{max}}$, $[P]$ is the protein concentration in tetramer, and K_d is the apparent dissociation constant in tetramer concentration. The maximum value was floated during the fitting.

IPTG Competition. The mutation of W220 causes a decrease of ~ 10 – 30 fold in the affinity of the repressor for inducer (40, 42) and removes the fluorescence signal most commonly used to monitor inducer binding (39). Therefore, the relative binding of inducer was monitored by following the decrease in operator binding in a nitrocellulose filter binding assay. For mutants with normal operator affinity, the concentration of operator was 5×10^{-12} M, and protein was 1.3×10^{-9} M tetramer. Protein concentration was increased to 2.6×10^{-8} M for mutants with a 10-fold decrease in operator binding affinity. IPTG concentration was varied over a range that spanned the apparent binding affinity. The operator and protein were preincubated in buffer for 15 min prior to addition of varying concentrations of IPTG. Samples were filtered, and counts retained were quantified and normalized as described for the operator binding assay. The amount of IPTG necessary to dissociate 50% of the operator–repressor complexes was determined by fitting the competition curves to the equation:

$$R = [\text{IPTG}]^n/(Y^n + [\text{IPTG}]^n) \quad (2)$$

where R is the fraction of bound complexes within each solution calculated by $R = \text{bound}/\text{bound}_{\text{max}}$, n is the “apparent” Hill coefficient, and Y is the amount of IPTG necessary to compete 50% of the operator–repressor complexes. The n value in this case reflects the need for more than one IPTG molecule to cause the *lac* repressor to dissociate from the operator.

¹ Abbreviations: DMSO, dimethyl sulfoxide; DTT, dithiothreitol; EDTA, ethylenediaminetetraacetic acid; IPTG, isopropyl β -D-thiogalactoside; SDS–PAGE, sodium dodecyl sulfate–polyacrylamide gel electrophoresis; Wless, *lac* repressor with W201Y and W220Y mutations.

Ammonium Sulfate Precipitation. This assay followed the protocol of Bourgeois (54) with the following modifications. The assay buffer used was 0.1 M Tris-HCl, pH 7.4, and 0.15 M KCl. Protein, ranging in concentrations from 1×10^{-6} to 1×10^{-5} M, was incubated with 15 mg/mL lysozyme and 5×10^{-7} M [14 C]IPTG for 5 min before precipitation with 70% saturated ammonium sulfate. The samples were centrifuged, the supernatants were removed, the pellets were resuspended in buffer, and the mixture was precipitated with 5% TCA. After centrifugation, the amount of radiolabel in the supernatant was determined by scintillation counting. For each condition, a duplicate sample was prepared with the addition of 1 mM IPTG to determine the level of nonspecific retention of [14 C]IPTG. The difference between the samples corresponds to the specific binding of the radiolabeled sugar.

Fluorescence Spectroscopy Measurements. Emission spectra were collected on an SLM 8100 spectrofluorometer. The protein was diluted to a final concentration of 5×10^{-7} M tetramer in TMS buffer (0.01 M Tris-HCl, pH 7.4, 0.2 M KCl, 0.01 M MgCl₂, 1 mM EDTA, and 0.1 mM DTT). The samples were excited at 295 nm, and emission spectra were collected from 300 to 400 nm. All spectra are noncorrected. These spectra were integrated for each mutant to determine the quanta emitted. The UV absorbance peak at 295 nm was measured on an SLM 3000 diode array spectrophotometer to determine the quanta absorbed. The quantum yield was determined by dividing the quanta emitted by the quanta absorbed. The values for the single tryptophan repressors were normalized to the wild-type value for comparison.

Circular Dichroism Spectroscopy. *Lac* repressor mutants were diluted to a concentration of 4×10^{-6} M monomer in 0.12 M potassium phosphate buffer, pH 7.4. Samples were scanned from 250 to 200 nm by an Aviv 62DS spectropolarimeter in a 1 cm path-length quartz cuvette. Data were collected for all mutants and compared to the wild-type spectrum.

Fluorescence Lifetimes. Fluorescence decay curves for the tryptophans in the mutant repressor proteins were collected on an SLM 48000 MHF phase/modulator frequency domain spectrofluorometer equipped with a 10 W argon laser (Coherent Inc.) with a deep UV output. The laser beam was modulated over a frequency range of 4–280 MHz by a Pockel's cell. Data were collected simultaneously at multiple frequencies and decomposed by means of Fourier transform. Samples were collected using an emission cut-on filter of 320 nm or, in a few cases, 340 nm. Proteins were diluted into 0.1 M Tris-HCl, pH 7.4 or 9.2, and 0.1 M KCl to a final concentration of 2 μ M monomer. Where ligands were present, samples contained a final concentration of 1×10^{-3} M IPTG or 1×10^{-6} M operator DNA for these studies. The intensity decay data between 4 and 116 MHz were analyzed as a Fourier transform in terms of the multiexponential decay law:

$$I(t) = I_0 \sum \alpha_i \exp(-t/\tau_i) \quad (3)$$

where I_0 has been set to unity, α_i and τ_i are the normalized preexponential factor and decay time associated with fluorescence component i , and t is time. The data are converted into f_i , the fractional intensity, by the relationship:

$$f_i = \alpha_i \tau_i / \sum \alpha_i \tau_i \quad (4)$$

Data analysis was performed with a nonlinear least squares

program from SLM and with the program Globals Unlimited (University of Illinois, Urbana, IL) (55). Values obtained from these two different analytical approaches were similar.

Fluorescence Quenching. Quenching experiments for *lac* repressor proteins were performed as described previously (42, 56). Stock solutions of potassium iodide, acrylamide, and thallium acetate were made at concentrations of 5, 4.2, and 5 M, respectively. Potassium iodide was prepared fresh each day in buffer with 1 mM sodium thiosulfate to inhibit production of I₂ (57). Thallium acetate was dissolved in water, and the acrylamide solution was purchased from National Diagnostic Inc. (58). Proteins were diluted to a concentration of 5×10^{-7} M monomer in 0.01 M Tris-HCl, pH 7.4 or 9.2, and 0.15 M KCl for the potassium iodide or acrylamide quenching. Samples for thallium acetate quenching were diluted into 0.05 M Tris-acetate, pH 7.4 or 9.2, and 0.15 M potassium acetate to avoid formation of insoluble thallium chloride. Samples with ligand contained a final concentration of 1×10^{-3} M IPTG or 5×10^{-7} M operator. Samples were excited at 285 nm, and the intensity was monitored at the emission wavelength peak for each mutant (Table 2). Aliquots of a stock solution of quenching agent (5 μ L per addition) were added until the final concentration of potassium iodide, acrylamide, or thallium acetate was 0.25, 0.2, or 0.25 M, respectively. Fluorescence intensity correction factors were generated using identical titrations with buffer for the potassium iodide and acrylamide samples. A 5 M potassium acetate stock was used to generate the correction factors for the thallium acetate experiments. Thallium acetate was insoluble at higher concentrations in pH 9.2, and no data could be collected for this condition.

RESULTS

Generation of Mutants and Protein Purification. Single tryptophan substitutions at residues Y7, L62, H74, E100, Q117, F226, Y273, F293, and K325 were generated in a "tryptophan-less" background of the double mutation, W201Y/W220Y (Wless). For each mutant, the entire *lacI* gene was sequenced to confirm that the three mutated residues were the only alterations in the DNA sequence. All mutant repressors were expressed in *E. coli* lacking the *lacI* gene and purified by phosphocellulose column chromatography. The purity was assessed by electrophoresis using 10% SDS-PAGE and visualized by silver staining as shown in Figure 1. E100/Wless and Q117/Wless were produced in low quantities and were not as pure as the remaining mutant repressor proteins. Circular dichroism spectra for all repressors demonstrated the same secondary structure content as wild type repressor within experimental error (data not shown). On the basis of gel filtration chromatography or elution behavior from the phosphocellulose column, all mutant proteins were deduced to be tetrameric (data not shown).

Functional Properties of Single Tryptophan Mutants. *Lac* repressor mutants possessing a single native tryptophan have been created previously (40, 42). As anticipated from previous studies, the W220Y mutation had minimal effect on operator binding but lowered the affinity for inducer (Table 1), and the W201Y mutation resulted in a 3-fold reduction in operator affinity but had minimal effect on inducer binding. The Wless mutant exhibits similar binding properties with a 10-fold decrease in inducer affinity and a 3-fold lower affinity for operator (Table 1). Therefore, the

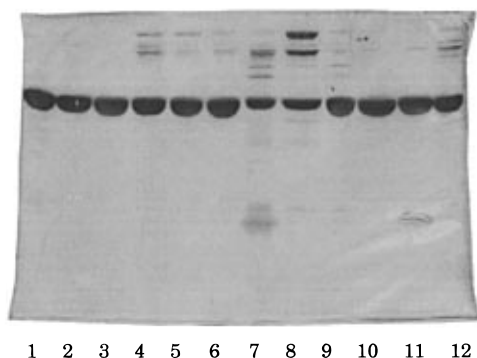


FIGURE 1: Purity of mutant repressor proteins. Protein purity was examined by electrophoresis on a 10% SDS-PAGE gel and visualized by silver stain. Ten micrograms of repressor protein was loaded for each lane: lane 1, wild type; lane 2, W201Y; lane 3, W220Y; lane 4, Y7W/Wless; lane 5, L62W/Wless; lane 6, H74W/Wless; lane 7, E100W/Wless; lane 8, Q117W/Wless; lane 9, F226W/Wless; lane 10, Y273W/Wless; lane 11, F293W/Wless; lane 12, K325W/Wless.

Wless mutation results in a *lac* repressor which binds operator and inducer with high affinity, exhibits inducer sensitivity for operator binding, and presumably undergoes a conformational change similar to that of the wild-type protein upon ligand binding.

Several of the single tryptophans introduced into the Wless background affect operator or inducer binding (Table 1). Inducer binding was monitored indirectly by the effect of IPTG on operator binding. The concentration of inducer required for 50% dissociation of the repressor-operator complex is reported in Table 1. The H74W/Wless mutant displays a 10-fold increase in affinity for operator and an apparent loss of inducer binding when measured in this assay. The L62W/Wless and K325W/Wless mutant proteins exhibit a reduction in operator affinity compared to the Wless background, and the Y7W/Wless protein does not recognize operator. The Q117W/Wless and F293W/Wless proteins cause a >10-fold decrease in apparent affinity for inducer and a return to wild-type operator affinity relative to the Wless background.

Although the specific mechanism may be unrelated, *lac* repressor wild-type protein at pH 9.2 mimics the functional properties of the operator-bound conformation (27, 28, 59). These properties consist of a 10-fold decrease in affinity and

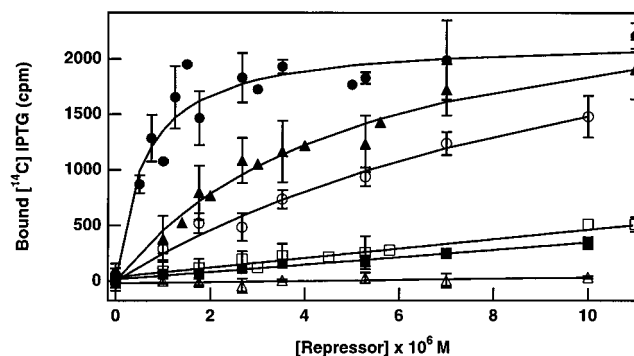


FIGURE 2: IPTG binding measured by ammonium sulfate assay. Binding was measured as described in Bourgeois (54) with modifications listed in Materials and Methods. Curves are drawn through the data for comparison purposes only. The different proteins are as follows: wild type (●), H74W (▲), W201Y/W220Y (○), H74W/Wless (□), F293W/Wless (■), and D274N with a C-terminal histidine tag (△). The D274N mutant of *lac* repressor displays no inducer binding (56).

cooperative binding of inducer. The operator dissociation assay cannot detect cooperativity at pH 9.2; however, the decrease in inducer affinity between pH 7.4 and pH 9.2 can be monitored. The only mutant protein in the Wless background which failed to show the expected decrease in affinity at pH 9.2 was E100W/Wless (Table 1). The Q117W/Wless repressor-operator complex was not dissociated by IPTG as efficiently as the otherwise comparable F293W/Wless repressor-operator complex at pH 9.2.

The H74W/Wless protein has perhaps the most interesting effect on function. The relative affinity of this protein for inducer could not be measured by operator dissociation because no effect on operator binding was observed at either pH examined. Even at IPTG concentrations of 800 mM or following extended incubation, no release of bound operator was observed. Therefore, an ammonium sulfate precipitation assay was used to determine if H74W/Wless mutant protein actually binds to inducer. The binding of inducer to wild-type protein and mutant repressors with different inducer binding affinities is shown in Figure 2. In this assay, the H74W/Wless protein displayed the same inducer binding as F293W/Wless. However, at the concentration of inducer adequate to dissociate operator from F293W/Wless, no decrease in operator binding was detected for H74W/Wless.

Table 1: Ligand Binding Properties of Single Tryptophan Proteins

repressor	K_d operator binding ^a ($\times 10^{11}$ M)	[IPTG] for 50% operator dissociation ^b	
		pH 7.4 ($\times 10^6$ M)	pH 9.2 ($\times 10^6$ M)
wild type	1.6 ± 0.1	3.6 ± 1	78 ± 10
W201Y	5.2 ± 0.9	1.5 ± 0.4	33 ± 4
W220Y	3.0 ± 0.6	29 ± 3	522 ± 80
Wless	5.4 ± 0.6	33 ± 5	363 ± 30
Y7W/Wless	nb ^c	nd ^d	nd
L62W/Wless	20 ± 3	23 ± 6	267 ± 30
H74W/Wless	0.51 ± 0.04	ni ^e	ni
E100W/Wless	5.2 ± 1	47 ± 9	75 ± 10
Q117W/Wless	1.6 ± 0.4	445 ± 100	>2000
F226W/Wless	4.8 ± 0.8	51 ± 10	564 ± 60
Y273W/Wless	7.0 ± 0.8	11 ± 3	150 ± 20
F293W/Wless	2.0 ± 0.2	520 ± 100	>2000
K325W/Wless	38 ± 10	17 ± 7	181 ± 70

^a The apparent dissociation constant for 40-bp operator DNA ($\sim 2 \times 10^{-12}$ M) was measured by nitrocellulose filter binding assay. Each value was determined by fitting at least three curves simultaneously to eq 1 in Materials and Methods. ^b The relative affinity of the protein for IPTG was determined by competition of repressor/operator complexes by the addition of IPTG. Each value was generated by fitting at least three curves simultaneously to eq 2 in Materials and Methods. Error values were generated by Igor Pro and represent the standard deviation of the fitted curve.

^c nb = no binding. ^d nd = not determined. ^e ni = no induction.

Table 2: Spectral Properties of Single Tryptophan Proteins^a

repressor	Φ^b	emission max (nm)	
			+IPTG
wild type	1.00	336	327
W201Y	0.65	338	329
W220Y	0.45	325	325
Y7W/Wless	0.29	336	336
L62W/Wless	0.27	336	336
H74W/Wless	0.39	348	343
E100W/Wless	0.23	335	335
Q117W/Wless	0.46	334	334
F226W/Wless	0.28	330	330
Y273W/Wless	0.46	338	332
F293W/Wless	0.36	329	325
K325W/Wless	0.31	337	337

^a Protein concentration was 5×10^{-7} M tetramer diluted in TMS buffer, pH 7.4. The samples were excited at 295 nm, and the emission maximum was the wavelength with the greatest intensity in the spectrum collected from 300 to 400 nm. The quantum yield was determined as described in Materials and Methods. ^b Relative quantum yield was determined by dividing the mutant repressor quantum yield by the wild-type quantum yield.

The inability of H74W/Wless to respond to inducer binding indicates that this repressor may assume irreversibly the conformation with high affinity for operator and diminished affinity for inducer.

Fluorescence Properties. Steady-state fluorescence spectra were determined for all single tryptophan repressors. The relative quantum yield and emission wavelength maximum are given in Table 2. A change in the polarity of the environment in which a tryptophan residue resides can result in a change in the emission wavelength. Mutants were screened for changes in their fluorescence spectrum in pH 9.2 buffer or in neutral buffer in the presence of saturating concentrations of ligand. No changes in any emission spectra were detected in the presence of operator or pH 9.2. However, the fluorescence spectra of a subset of the single tryptophan repressors were affected by inducer as shown in Figure 3. The W201Y mutant displays a 10 nm blue shift

in emission wavelength and a slight increase in intensity in the presence of inducer (40–42). Sommer et al. (40) suggested that this increase in intensity is a result of inducer initiating resolubilization of *lac* repressor which had aggregated during freeze/thaw conditions. The mutants H74W/Wless, Y273W/Wless, and F293W/Wless all shift to the blue end of the spectrum and show a decrease in intensity in the presence of inducer.

Time-Resolved Fluorescence. The fluorescence lifetime values for the single tryptophan mutants under different conditions are listed in Table 3. The exponential decays for *lac* repressor wild type and the two “native” single tryptophan mutants were best fit to two lifetimes, as observed previously (60, 61). The observed changes in the lifetime values for wild type and W201Y (W220 present) in the presence of inducer were also consistent with those previously published. The decrease in the lifetime of W220 in the inducer-bound form was attributed to contacts with the sulfur of the inducer molecule (61). All of the single tryptophan mutants were best fit to a model with four lifetimes. The longest and shortest lifetimes were not well determined. Both H74W/Wless and Y273W/Wless lifetimes decreased in the presence of inducer, as shown in Figure 4. Interestingly, the tryptophan at F293, a residue which forms hydrophobic interactions with inducer similar to those formed by W220 in the crystallographic structure, does not display the long lifetime of W220, nor does its lifetime change in the presence of inducer. The presence of multiple lifetimes for the mutant repressors may indicate that these tryptophans are in areas which exist in multiple conformations or that the mutation of the native tryptophans has created a protein which exists in additional conformational states.

Fluorescence Quenching. The exposure of the single tryptophan moiety in different conditions for each of the mutant proteins was measured by using neutral, anionic, and cationic quenchers. The Stern–Volmer and quenching rate constants were determined for all conditions and are summarized in Table 4. Linear Stern–Volmer plots (linear

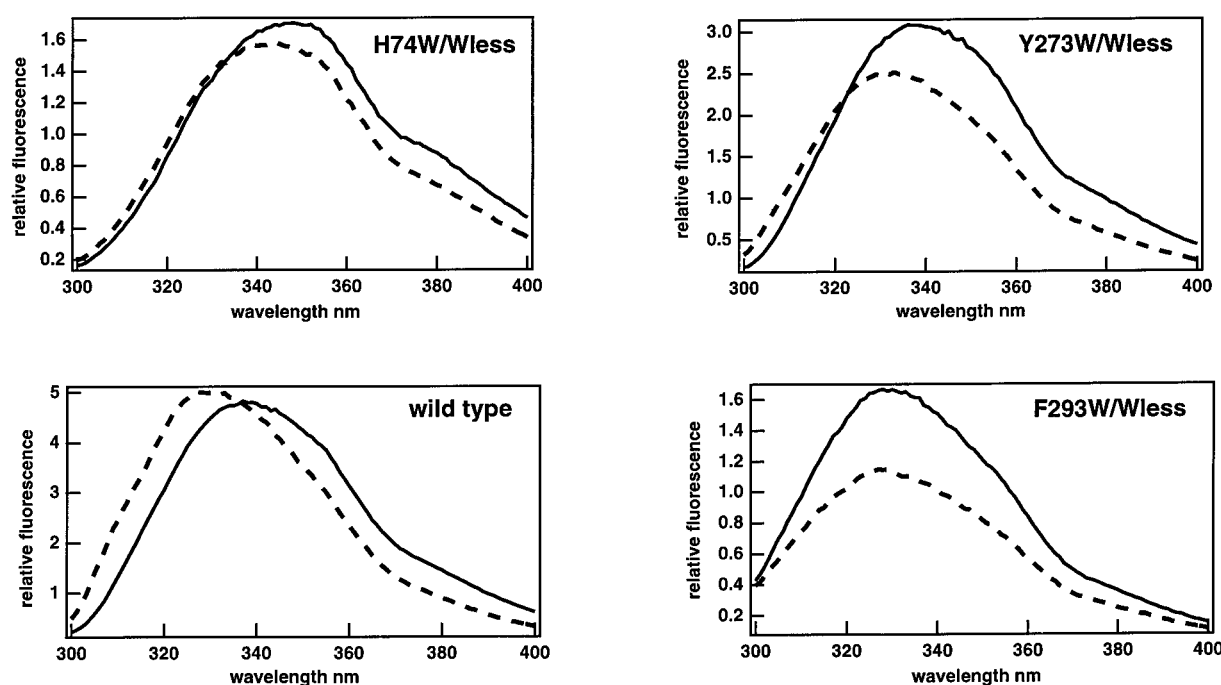


FIGURE 3: Fluorescence emission spectra of single tryptophan repressors. The repressor samples were diluted to 5×10^{-7} M tetramer in TMS buffer, pH 7.4, and excited at 295 nm. The emission spectra were collected from 300 to 400 nm and are represented by a solid line (—). The inducer-bound samples contain 1×10^{-3} M IPTG and are represented by a dashed line (---).

Table 3: Lifetimes of Single Tryptophan Proteins under Various Conditions^a

repressor	condition					
	pH 7.4		+IPTG		pH 9.2	
	τ^b	f^c	τ	f^c	τ	f^c
wild type	9.0 ± 0.2	0.88 ± 0.01	7.0 ± 0.2	0.90 ± 0.01	9.1 ± 0.1	0.88 ± 0.01
W201Y	2.1 ± 0.4	0.12 ± 0.01	1.6 ± 0.3	0.10 ± 0.02	2.0 ± 0.2	0.12 ± 0.01
	8.9 ± 0.2	0.92 ± 0.01	7.0 ± 0.8	0.93 ± 0.02	8.7 ± 0.2	0.92 ± 0.03
W220Y	1.6 ± 0.6	0.08 ± 0.01	1.1 ± 0.5	0.07 ± 0.02	1.4 ± 0.4	0.08 ± 0.03
	6.3 ± 0.4	0.84 ± 0.04	5.7 ± 0.4	0.90 ± 0.04	5.6 ± 0.2	0.90 ± 0.01
Y7W/Wless	1.0 ± 0.4	0.16 ± 0.04	1.1 ± 0.8	0.10 ± 0.04	0.61 ± 0.01	0.10 ± 0.01
	5.6 ± 0.4	0.48 ± 0.02	5.4 ± 0.6	0.50 ± 0.04	5.3 ± 0.2	0.48 ± 0.02
L62W/Wless	1.9 ± 0.2	0.36 ± 0.02	1.8 ± 0.3	0.34 ± 0.06	1.7 ± 0.1	0.34 ± 0.02
	<10 ps	0.10 ± 0.05	<10 ps	0.09 ± 0.05	<10 ps	0.12 ± 0.01
H74W/Wless	6.1 ± 0.6	0.58 ± 0.10	5.8 ± 0.1	0.51 ± 0.03	6.4 ± 0.1	0.46 ± 0.01
	2.1 ± 0.8	0.28 ± 0.06	2.3 ± 0.8	0.29 ± 0.01	2.3 ± 0.1	0.31 ± 0.01
E100W/Wless	<180 ps	0.10 ± 0.06	<250 ps	0.14 ± 0.04	<100 ps	0.18 ± 0.01
	8.6 ± 0.3	0.66 ± 0.03	7.7 ± 0.5	0.62 ± 0.03	8.6 ± 0.4	0.69 ± 0.03
Q117W/Wless	2.3 ± 0.4	0.23 ± 0.03	2.4 ± 0.3	0.26 ± 0.02	2.0 ± 0.2	0.20 ± 0.01
	<100 ps	0.07 ± 0.03	<100 ps	0.08 ± 0.01	<100 ps	0.09 ± 0.02
F226W/Wless	6.6 ± 0.7	0.42 ± 0.03	6.3 ± 0.2	0.42 ± 0.07	6.1 ± 0.3	0.42 ± 0.01
	2.3 ± 0.9	0.43 ± 0.02	1.8 ± 0.1	0.43 ± 0.02	1.7 ± 0.2	0.41 ± 0.01
Y273W/Wless	<350 ps	0.13 ± 0.04	<100 ps	0.12 ± 0.05	<100 ps	0.14 ± 0.02
	6.7 ± 0.5	0.60 ± 0.02	6.5 ± 0.2	0.59 ± 0.02	6.5 ± 0.3	0.64 ± 0.02
Y293W/Wless	2.3 ± 0.7	0.29 ± 0.03	2.1 ± 0.1	0.29 ± 0.02	2.1 ± 0.3	0.26 ± 0.02
	<190 ps	0.09 ± 0.01	<100 ps	0.10 ± 0.02	<50 ps	0.08 ± 0.01
K325W/Wless	5.6 ± 1.0	0.58 ± 0.02	5.0 ± 0.8	0.60 ± 0.01	5.0 ± 0.02	0.60 ± 0.01
	2.3 ± 0.6	0.30 ± 0.04	1.8 ± 0.2	0.27 ± 0.02	2.0 ± 0.08	0.25 ± 0.01
Y273W/Wless	<180 ps	0.10 ± 0.04	<10 ps	0.10 ± 0.03	<10 ps	0.10 ± 0.02
	6.2 ± 0.3	0.76 ± 0.01	4.5 ± 0.40	0.75 ± 0.01	6.3 ± 0.3	0.78 ± 0.00
Y293W/Wless	2.6 ± 0.3	0.20 ± 0.01	1.8 ± 0.11	0.19 ± 0.01	2.5 ± 0.2	0.17 ± 0.00
	<10 ps	0.03 ± 0.02	<20 ps	0.05 ± 0.02	<10 ps	0.04 ± 0.01
K325W/Wless	5.9 ± 1.2	0.48 ± 0.03	5.8 ± 0.7	0.43 ± 0.02	5.7 ± 0.9	0.41 ± 0.03
	2.2 ± 0.9	0.35 ± 0.04	1.5 ± 0.1	0.36 ± 0.02	1.9 ± 0.2	0.41 ± 0.01
K325W/Wless	<250 ps	0.12 ± 0.03	<10 ps	0.17 ± 0.01	<70 ps	0.15 ± 0.02
	6.5 ± 0.5	0.46 ± 0.18	6.5 ± 0.4	0.40 ± 0.06	6.4 ± 0.4	0.44 ± 0.04
K325W/Wless	1.9 ± 0.4	0.31 ± 0.09	1.9 ± 0.06	0.35 ± 0.04	1.8 ± 0.1	0.31 ± 0.03
	<60 ps	0.22 ± 0.03	<20 ps	0.20 ± 0.06	<10 ps	0.21 ± 0.05

^a Single curves were analyzed for multiple lifetime components as described in Materials and Methods. The values are an average of three to eight determinations, and standard deviations are shown. The repressor concentration was 2×10^{-6} M monomer, and where present, the IPTG concentration was 1×10^{-3} M. Four lifetime components were required to achieve optimal fits for the mutant repressors in the Wless background; however, the longest lifetime component (>40 ns) was not well determined by the analyses and contributed $<7\%$ to the fluorescence intensity; therefore, this component is not reported. The shortest lifetime component was also not well determined and is reported as a value less than the mean value obtained. For computation of τ_{av} for determination of k_q (see Table 4), the longest lifetime component was eliminated from the calculation. Lifetimes were collected for all repressors in the presence of 1×10^{-6} M operator DNA (equivalent to the dimer concentration); however, no change in lifetime was detected for any mutant repressor compared to the pH 7.4 values, and these values are not reported. ^b τ is the lifetime in nanoseconds except where indicated. ^c f is the fractional intensity of each lifetime calculated according to eq 4 in Materials and Methods.

correlation coefficients >0.99) indicated that no static quenching occurred (62). The iodide and acrylamide quenching of wild-type and the native single tryptophan proteins correlated well with previous studies conducted under saturating concentrations of IPTG (40–42).

Iodide can quench only those tryptophans which are located near the surface of the protein due to its large size and negative charge. The single tryptophan mutants Y7W/Wless, L62W/Wless, E100W/Wless, Q117W/Wless, and K325W/Wless have Stern–Volmer constants greater than 1 and are highly exposed to solvent. The mutants H74W/Wless, F226W/Wless, and W201Y (W220 present) have intermediate quenching constants with partially exposed tryptophans residues. Tryptophans at sites buried in the structure, Y273W/Wless and W220Y (W201 present), are not quenched by iodide. In contrast, the low exposure to iodide quenching observed for the F293W/Wless protein is not consistent with its placement in the inducer binding pocket in the crystallographic structure (9, 10).

In the presence of saturating ligands, no changes are detected under any conditions for the mutant repressor proteins in which tryptophans are highly exposed to iodide. These residues may be too exposed to act as conformational

probes, and no conclusions about structural or environmental changes in these regions can be drawn. Similarly, measurement of iodide quenching with and without ligands did not detect any change in the exposure of the buried residues; however, iodide may be too large to penetrate and probe these areas. The only ligand to produce a change in the exposure of intermediately buried tryptophans was inducer. In the presence of inducer, H74W/Wless was less exposed to iodide and F293W/Wless was more exposed. As determined previously, both wild type and W201Y are less exposed to iodide in the presence of inducer (40, 42).

Acrylamide is a small neutral quencher that has the ability to penetrate the interior of the protein. The results of acrylamide quenching correlate with iodide quenching; exposed mutants have acrylamide Stern–Volmer constants greater than 7, moderately exposed mutants have acrylamide Stern–Volmer constants between 7 and 4, and the buried residues are less than 4. The F293W/Wless protein is moderately exposed to acrylamide in contrast to its low exposure to iodide and demonstrates no change of exposure in the presence of inducer. The wild-type, W201Y, and H74W/Wless proteins exhibit lower Stern–Volmer constants in the presence of inducer. However, the rate of quenching,

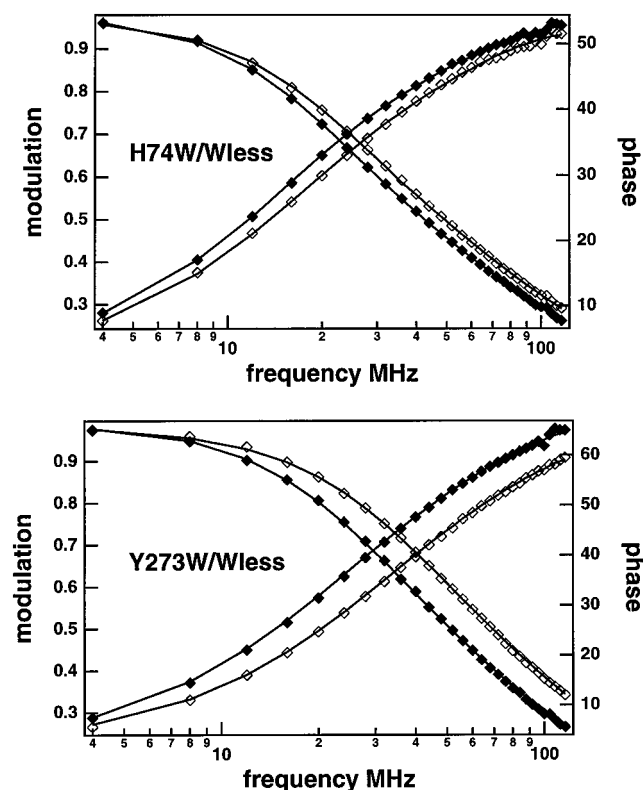


FIGURE 4: Phase/modulation fluorescence lifetime data for mutant repressor proteins. Protein concentration was 2 μ M monomer in 0.1 M Tris-HCl, pH 7.4, and 0.15 M KCl at 20 $^{\circ}$ C. Open symbols are data collected in the presence of 1×10^{-3} M IPTG. The solid lines are a fit to a four-exponential decay (eq 3) using Globals Unlimited (55) as described in Materials and Methods.

k_q , does not change due to a decrease in the lifetime of the tryptophan in the presence of IPTG. Bandyopadhyay and Wu (41) reported the same result for wild-type and W201Y mutant repressor proteins. For Y273W/Wless, the Stern-Volmer constant remains the same in the presence of inducer, but the decrease in the tryptophan lifetime results in an increase in the rate constant for quenching.

Thallium is a large, positively charged quencher that can be used to assess whether inconsistencies between iodide and acrylamide quenching are a result of a charged amino acid in the area. While other quenchers detected no changes in exposure in the presence of ligands for Y273W/Wless, exposure to thallium was decreased in the presence of both operator and inducer. In the presence of inducer, the F293W/Wless protein was less exposed to thallium. Therefore, the iodide and thallium quenchers, which have opposite charges, demonstrate different exposures for the F293W/Wless tryptophan residue. This result indicates that a charged residue may be in the vicinity of this tryptophan. No changes in the exposure of wild type, W201Y, or H74W/Wless were detected by thallium in the presence of inducer.

DISCUSSION

Conformational Changes Associated with Ligand Binding. While operator and inducer bind to the *lac* repressor at separate functional sites within the structure, the affinities for these ligands are nonetheless reciprocally related, presumably via conformational shifts in the protein in different ligand-bound states (1). These conformational changes associated with ligand binding in *lac* repressor have been explored previously by determining the accessibility of

residues to chemical modification (31–34), detecting spectral changes in tryptophan and tyrosine residues (36, 63–65), and other biophysical properties, in particular sedimentation constants (35). In temperature jump experiments, the presence of IPTG or protons affected the equilibrium of the conformational transition (43). Changes in spectral properties and chemical modification of lysines, tryptophans, and cysteines indicated that conformational changes occurred in the core region upon IPTG binding (31, 32, 34, 37, 38, 63–67). Both specific and nonspecific DNA binding also caused changes in the chemical modification of amino acid side chains and in the spectral properties of the modified residues (32–34, 38, 68). Since binding different ligands altered the pattern of modification or resulted in spectral changes in comparison with the unliganded form, *lac* repressor was hypothesized to exist in two extreme conformations, with the unliganded form in equilibrium between the operator- and inducer-bound conformations (28, 39, 43). The availability of the crystallographic structures for free protein and both ligand-bound states provides the opportunity to identify regions that may contribute to linking these functions or may be affected by the conformational alterations associated with binding (9, 10). Surprisingly, in contrast to the multiple changes observed upon inducer binding in the spectral properties and reactivity of side chains to chemical modification, the free and inducer-bound forms of the protein were found to be very similar in the crystal structure, while the operator-bound form displayed changes in orientation of the N-subdomain of the core region.

Tryptophan Scanning Mutagenesis To Probe Local Environment. The sensitivity of tryptophan fluorescence to the surrounding environment provides a mechanism to detect structural changes occurring in the presence of different ligands and has led to intense study of the native tryptophans in the *lac* repressor protein. The location of W201 in the interior of the C-subdomain and W220 in the inducer binding site by genetic and biochemical studies (39, 40, 42, 66) has been confirmed by the crystallographic structures (9, 10). The diminished inducer affinity caused by the W220Y mutation and all mutants containing this alteration can be expected on the basis of the role of this side chain in binding to inducer. By selective substitution of single tryptophans in a Wless background (W201Y/W220Y), different regions of the protein can be monitored specifically and exclusively to explore the dynamic events responsible for the mutual influence of different ligands on functional properties and on the conformation of the *lac* repressor protein (Figure 5). Since these tryptophans have been introduced into the structure in place of the native amino acid, the data must be interpreted in the context of effects that derive from altering the specific amino acid as well as from the steric influence of the bulky indole side chain. Multiple amino acid substitutions for different residues of *lac* repressor have been analyzed for their *in vivo* phenotype in previous studies (14). These studies include substitutions of alanine, tyrosine, and phenylalanine for all the residues analyzed in these experiments except H74. In the ensuing discussion, the effects of these substitutions on *lac* repressor function *in vivo* will be compared to the *in vitro* results for the single tryptophan mutants.

Exposed Tryptophan Side Chains in Single Mutants Unaffected by Ligand, While Spectral Properties of Buried Residues Altered. The single tryptophan mutants generated in this study can be grouped into two categories: exposed

Table 4: Quenching Properties of Single Tryptophan Proteins^a

repressor	condition	iodide		acrylamide		thallium	
		K_{sv} (M ⁻¹)	k_q (M ⁻¹ s ⁻¹)	K_{sv} (M ⁻¹)	k_q (M ⁻¹ s ⁻¹)	K_{sv} (M ⁻¹)	k_q (M ⁻¹ s ⁻¹)
wild type	pH 7.4	0.84	0.10	5.4	0.66	1.9	0.23
	+IPTG	0.29	0.05	4.3	0.67	2.0	0.31
	pH 9.2	0.72	0.09	5.5	0.67		
W201Y	+DNA	0.84	0.10	5.1	0.65	1.1	0.14
	pH 7.4	1.1	0.13	6.0	0.72	1.7	0.20
	+IPTG	0.5	0.08	4.6	0.70	1.1	0.17
W220Y	pH 9.2	0.9	0.11	7.5	0.93		
	+DNA	1.3	0.15	8.0	0.95	1.5	0.18
	pH 7.4	nq ^b (0.01)		2.1	0.39		
Y7W/Wless	+IPTG	nq (0.01)		2.2	0.42		
	pH 9.2	nq (0.01)		2.4	0.47		
	+DNA	nq (0.01)		2.4	0.45		
L62W/Wless	pH 7.4	1.5	0.45	7.8	2.3		
	+IPTG	1.4	0.42	8.1	2.4		
	pH 9.2	1.4	0.45	7.6	2.5		
H74W/Wless	+DNA						
	pH 7.4	1.2	0.29	8.2	2.0		
	+IPTG	1.1	0.30	8.3	2.3		
E100W/Wless	pH 9.2	1.2	0.32	6.9	1.9		
	+DNA	1.3	0.37	7.2	2.0		
	pH 7.4	0.43	0.07	6.6	1.1	7.6	1.2
Q117W/Wless	+IPTG	nq (0.02)		5.2	0.96	7.8	1.4
	pH 9.2	0.23	0.04	6.5	1.0		
	+DNA	0.38	0.07	5.8	1.0	7.4	1.3
F226W/Wless	pH 7.4	1.6	0.42	7.5	2.0		
	+IPTG	1.6	0.46	8.5	2.5		
	pH 9.2	1.4	0.43	7.0	2.1		
Y273W/Wless	+DNA	1.3	0.37	6.8	1.9		
	pH 7.4	1.4	0.30	8.1	1.7		
	+IPTG	1.5	0.34	7.9	1.8		
F293W/Wless	pH 9.2	1.4	0.30	8.2	1.7		
	+DNA	1.2	0.27	8.3	1.8		
	pH 7.4	0.47	0.12	5.4	1.4		
K325W/Wless	+IPTG	0.42	0.12	5.7	1.6		
	pH 9.2	0.41	0.12	5.4	1.5		
	+DNA	0.46	0.13	5.9	1.7		
Y273W/Wless	pH 7.4	nq (0.1)		3.3	0.63	2.0	0.38
	+IPTG	nq (0.1)		3.7	0.99	0.96	0.26
	pH 9.2	nq (0.2)		3.4	0.64		
F293W/Wless	+DNA	nq (0.2)		3.6	0.74	0.90	0.19
	pH 7.4	nq (0.2)		5.8	1.6	6.3	1.7
	+IPTG	0.34	0.11	5.3	1.7	2.2	0.72
K325W/Wless	pH 9.2	nq (0.01)		4.9	1.6		
	+DNA	nq (0.1)		5.6	1.8	6.2	2.0
	pH 7.4	1.1	0.30	9.0	2.5		
K325W/Wless	+IPTG	1.1	0.33	8.4	2.6		
	pH 9.2	1.3	0.39	9.2	2.7		
	+DNA	1.3	0.38	8.7	2.6		

^a The K_{sv} values shown are calculated from the equation $F_0/F = 1 + K_{sv}[Q]$, where F_0 is the fluorescence intensity at the emission peak maximum before addition of quencher, F is the intensity after addition of quencher, $[Q]$ is the concentration of quencher, and K_{sv} is the Stern–Volmer constant. The quenching rate, k_q , is calculated using the relationship $k_q = K_{sv}/\tau_{av}$. The average lifetime, τ_{av} , was calculated from $\tau_{av} = \sum f_i \tau_i$ using the lifetime data reported in Table 3. All quenching values are an average of two to four replicates, and the standard deviation for all conditions did not exceed 35% of the reported value, with the exception of thallium acetate quenching for wild-type protein, which had a standard deviation of 50%. The linear correlation coefficient for all plots was >0.99 except for the potassium iodide experiments which displayed low Stern–Volmer constants. All conditions that demonstrated a change in quenching as reported in the text were measured at least three times. ^b nq = not quenched. Not quenched was defined as any sample with an iodide quenching constant ≤ 0.2 . Approximate values for these conditions are reported in parentheses.

and buried. Based upon the emission wavelength and quenching data, the substitutions of Y7W/Wless, L62W/Wless, E100W/Wless, Q117W/Wless, and K325W/Wless all generate exposed tryptophan residues. These proteins display large Stern–Volmer quenching constants with both iodide and acrylamide and an emission spectrum with its peak at ~ 336 nm. Except for Q117, all these residues were predicted to be exposed on the basis of inspection of the X-ray crystallographic structures (9, 10) and confirmed by analysis of genetic and structural data by Suckow et al. (69). The substitutions that produced proteins with tryptophans not exposed to solvent, H74W/Wless, Y273W/Wless, and F293W/

Wless, exhibited altered spectra and changed quenching properties in the presence of inducer. The spectral and functional properties of these single tryptophan repressors will be examined individually.

No Spectral Alterations for Exposed Tryptophans at E100 and Q117 Despite Placement in Region of Significant Structural Change. The most significant rearrangement between the structures of the different liganded states of *lac* repressor results from a rotation of the monomers relative to each other in the monomer–monomer interface of the N-subdomain of the core (see Figure 5). Two residues (E100 and Q117) present in this N-subdomain interface were

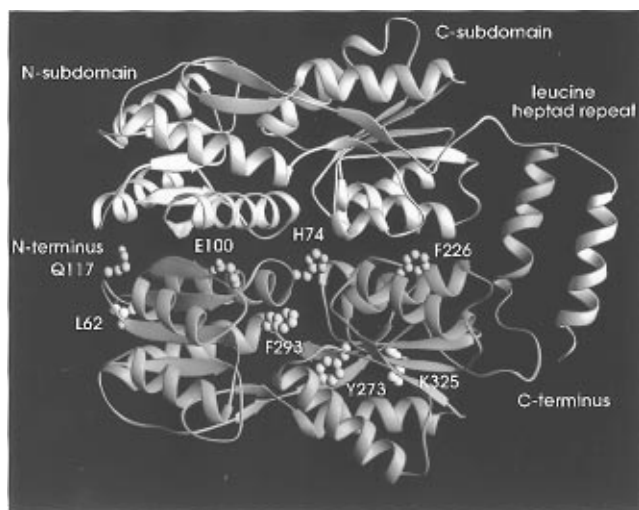


FIGURE 5: *Lac* repressor core domain structure with residues substituted by tryptophan. Only one dimer of the tetrameric structure is shown. The structure of the dimer *lac* repressor core region bound to inducer was derived from PDB file 1LBH (10). One monomer is represented in green and the other monomer is colored blue. The figure was drawn in Ribbons version 2.63 (71). The residues substituted with tryptophan residues are shown in one of the monomers. The monomer–monomer interface residues (H74, E100, Q117, and F226) are colored red, the interior residues (Y273 and F293) are colored rose, and the exposed residues (L62 and K325) are colored gold. The Y7 residue is not shown because this region of the protein is not resolved in the crystal structure of the repressor–inducer complex. The N- and C-termini, the N- and C-subdomains, and the leucine heptad repeat sequences of this structure are labeled.

mutated to tryptophan in the Wless background. In the inducer-bound structure, E100 is in contact with K84 across the dimer interface of its partner monomer (10). No amino acid substitutions for E100 altered the function of the protein in the previous phenotypic analyses (14). However, mutation of K84 to glutamate or arginine results in a loss of pH sensitivity for inducer binding (17), a result also seen with substitution of tryptophan for E100. Thus, this partner pair appears to be involved in the pH-associated allostery observed for inducer binding.

In the inducer-bound form, Q117 makes contact across the interface with R118 of the partner monomer (10). Either disruption of this contact or introduction of the bulky tryptophan side chain resulted in a decrease in the affinity for inducer. Although phenotypic assays indicated that mutation to alanine, phenylalanine, and tyrosine at Q117 did not alter the inducer binding properties, alanine substitution resulted in decreased repression. The bulk of the indole side chain may affect the functional properties of the Q117W/Wless mutant. These mutants emphasize the ability of amino acids not in the binding region to affect ligand binding. In this case, mutation of Q117 to tryptophan, which is located further from the inducer binding site, has a greater impact on inducer binding than mutation of E100. The tryptophans substituted in this interface were exposed and demonstrated no change in environment in the presence of ligands. The exposure of these residues could derive from the need for spatial flexibility in this interface to produce conformational change in this region. Alternatively, the large tryptophan residue may be extruded toward solvent due to steric constraints.

Substitutions Y7W, L62W, and K325W Affect Operator Binding without Spectral Change. The remaining exposed tryptophan substitution mutant proteins, Y7W/Wless, L62W/

Wless, and K325W/Wless, all exhibited altered operator affinity and no change in fluorescence properties upon ligand binding. In the wild-type protein, Y7 is in the DNA binding region as part of the helix–turn–helix motif. While no contact is made by Y7 with operator, this residue positions Y17 to make specific operator–protein contacts (70). Mutation of this residue to alanine and phenylalanine resulted in decreased repression in previous phenotypic assays (14). In the wild-type protein, L62 is located between the operator binding region and the core domain in the structure (9, 10). Alanine, tyrosine, and phenylalanine substitutions at this site result in wild-type phenotypic behavior (14). This area appears sufficiently flexible for a tryptophan substitution, but the bulky tryptophan residue may perturb the spacing of the N-subdomain and DNA binding headpieces with a consequent decrease in operator affinity.

In the wild-type protein, K325 is in the area where the C-subdomain links to the leucine heptad repeats of the dimer–dimer interface. This region is important for maintaining the structural integrity of the C-subdomain, and a reduction in operator affinity may result from destabilization of the overall monomer structure. Mutants of the adjacent residue R326 also resulted in a loss of operator affinity (51); however, no amino acid substitutions for the K325 residue display an altered phenotype (14).

Tryptophan Substitution at H74 Abolishes Inducibility and Demonstrates Spectral Response to Inducer Binding in This Region. In the crystal structure of wild-type *lac* repressor bound to inducer, H74 is located in the N-subdomain in the monomer–monomer interface and forms an electrostatic interaction across this interface with D278 in the C-subdomain of its partner monomer. In the operator-bound structure of the protein, rearrangement of the monomer–monomer interface disrupts this contact due to the distance between these two residues (10). Placement of a tryptophan at this site decreases inducer affinity, enhances operator affinity, and results in a loss of induction. Whether these results are unique to altering the specific side chain at position 74 or derive from placing a bulky tryptophan in this region is uncertain. No protein production was observed for the D278W/Wless mutation (Barry and Matthews, unpublished results), further suggesting the importance of this interaction. Although the communication between operator and inducer binding sites has been disrupted, the fluorescence properties of H74W/Wless were nonetheless altered in the presence of inducer. The shift of the fluorescence emission spectrum to a shorter wavelength and decreased exposure to iodide indicates that tryptophan at this site is less exposed in the presence of inducer. Thus, introduction of tryptophan at position 74 generates a protein that does not release operator in response to inducer binding but still displays alterations in environment associated with inducer binding. This region may be crucial in the conformational alterations that accompany inducer binding.

Fluorescence Properties of Tryptophan at Position 273 Affected by Inducer and Operator Binding. The residue Y273 is located near the inducer binding cleft in the C-subdomain but is not directly involved in binding inducer (9, 10). However, the tryptophan residue substituted at position 273 has its emission spectra, lifetime, and accessibility to quencher altered in the presence of inducer. In the presence of inducer, the tryptophan at this position is less exposed to thallium but displays an increased exposure to acrylamide quenching. A similar decrease in exposure

may occur for iodide quenching, but the very low accessibility of this tryptophan to iodide precludes accurate analysis. A decrease in exposure to thallium quenching was also detected in the presence of operator. Although residue 273 is not located in the operator binding region, the substitution of tryptophan at this position causes a slight decrease in operator affinity. Previous phenotypic analysis of Y273 substituted by alanine, serine, or glycine demonstrated loss of inducer binding, and substitution by glutamine, arginine, proline, glutamate, or lysine resulted in diminished repression (14). However, substitution of phenylalanine or leucine for Y273 yielded proteins with wild-type function (14). These results indicate that subtle changes in the region of the structure between the inducer binding cleft and the C-subdomain occur in the presence of both inducer and operator.

Fluorescence Properties of Tryptophan at Position 293 Altered by Inducer Binding. In the wild-type protein, F293 is located at the end of the second crossover helix in the N-subdomain. In previous phenotypic assays, conversion of F293 to alanine resulted in weaker inducer binding, while tyrosine substitution greatly decreased inducer binding (14). Mutation to an even bulkier tryptophan residue significantly diminished inducer binding in our *in vitro* assays. F293 is part of a hydrophobic patch, including W220, that participates in inducer binding (9, 10). The fluorescence emission spectra of the tryptophans at W220 and F293 shift to a shorter wavelength in the presence of inducer, indicating that inducer shields them from solvent. However, W220 and F293 are located at opposite ends of the inducer binding pocket, and the other fluorescence properties of these tryptophan residues display different responses to inducer binding. Unlike W220 and the tryptophan substituted for H74 or Y273, there is no lifetime decrease upon inducer binding for the tryptophan at F293. In addition, the quenching behavior for the tryptophans at 220 and 293 differs in the presence of inducer. Accessibility of quenchers to the tryptophan at F293 in the presence of inducer depended upon the charge of the large quenching agents. The presence of inducer increases accessibility to iodide and decreases accessibility to thallium. Complexed to inducer, W220 is less exposed to iodide but displays no change in exposure to thallium quenching. This comparison of the fluorescence properties of W220 and F293W/Wless indicates that there are charge and steric differences in their locations in the inducer binding pocket.

Tryptophan Substituted at Position 226 Is Partially Buried and Unresponsive to Ligand Binding. The tryptophan substitution at residue F226 is the only partially buried tryptophan whose fluorescence properties were not affected by ligand binding. This result is consistent with the C-subdomain of the monomer–monomer interface being generally more immobile during ligand-induced conformational changes (10). In the crystal structure, residue F226 participates in a hydrophobic patch that preserves the stability of the dimer interface, and the substitution of a tryptophan does not appear to perturb this function. In previous phenotypic assays, substitution at this residue by alanine, tyrosine, or phenylalanine did not alter the functional properties of the protein (14).

Conclusion. The results with *lac* repressor illustrate the different types of information that can be derived using the sensitivity of tryptophan fluorescence to environmental changes. The combination of genetic studies with the availability of multiple crystal structures has led to the

development of a model for conformational change that occurs upon ligand binding to *lac* repressor (9, 10, 14, 69). The crystal structures of *lac* repressor in free versus operator-bound states display a rotation of the monomers relative to each other in the N-subdomain of the subunit interface. This rearrangement breaks contacts that H74 makes with its partner monomer in the unliganded form. In contrast, minimal changes are seen between free and inducer-bound structures. The fluorescence properties of H74W/Wless were unaffected by operator binding; however, inducer binding elicited changes in fluorescence lifetime and in accessibility to different quenchers. Even with the inability of inducer binding to effect operator release in this mutant protein, the fluorescence data demonstrate structural changes between the unliganded protein and the inducer-bound protein that are not readily evident in a comparison of the wild-type crystal structures.

By judicious selection of sites for tryptophan substitution, additional insight into conformational states and the influence of ligands can be obtained by fluorescence spectroscopy. However, structural shifts that affect completely exposed or buried residues may not elicit sufficient change in the environment to alter the fluorescence properties of the tryptophan. For example, the tryptophans substituted in the N-subdomain monomer–monomer interface for E100 or Q117 may be solvent exposed and/or extrude the large hydrophobic side chain into solvent to maintain this interface. Thus, the types of changes which can be monitored by tryptophan probes are selective and depend on local environment, role of the residue, and solvent accessibility. In the case of the *lac* repressor, the residues that yielded significant information were in the central region of the protein proximal to the inducer binding site and were influenced almost exclusively by inducer binding.

ACKNOWLEDGMENT

The advice of Drs. Catherine Royer and Ross Reedstrom on the analysis of the fluorescence lifetime data and assistance from Tod Romo in generating the figures for the manuscript are gratefully acknowledged.

REFERENCES

1. Miller, J. H., and Reznikoff, W. S. (1980) *The Operon*, 2nd ed., Cold Spring Harbor Laboratory, Cold Spring Harbor, NY.
2. Gilbert, W., and Müller-Hill, B. (1966) *Proc. Natl. Acad. Sci. U.S.A.* 56, 1891–1898.
3. Riggs, A. D., and Bourgeois, S. (1968) *J. Mol. Biol.* 34, 361–364.
4. Alberti, S., Oehler, S., von Wilcken-Bergmann, B., Krämer, H., and Müller-Hill, B. (1991) *New Biol.* 3, 57–62.
5. Chakerian, A. E., Tesmer, V. M., Manly, S. P., Brackett, J. K., Lynch, M. J., Hoh, J. T., and Matthews, K. S. (1991) *J. Biol. Chem.* 266, 1371–1374.
6. Chen, J., and Matthews, K. S. (1992) *J. Biol. Chem.* 267, 13843–13850.
7. Alberti, S., Oehler, S., von Wilcken-Bergmann, B., and Müller-Hill, B. (1993) *EMBO J.* 12, 3227–3236.
8. Chen, J., Surendran, R., Lee, J. C., and Matthews, K. S. (1994) *Biochemistry* 33, 1234–1241.
9. Friedman, A. M., Fischmann, T. O., and Steitz, T. A. (1995) *Science* 268, 1721–1727.
10. Lewis, M., Chang, G., Horton, N. C., Kercher, M. A., Pace, H. C., Schumacher, M. A., Brennan, R. G., and Lu, P. (1996) *Science* 271, 1247–1254.
11. Platt, T., Files, J. G., and Weber, K. (1973) *J. Biol. Chem.* 248, 110–121.

12. Müller-Hill, B. (1975) *Prog. Biophys. Mol. Biol.* 30, 227–252.
13. Miller, J. H. (1979) *J. Mol. Biol.* 131, 249–258.
14. Kleina, L. G., and Miller, J. H. (1990) *J. Mol. Biol.* 212, 295–318.
15. Schmitz, A., Schmeissner, U., Miller, J. H., and Lu, P. (1976) *J. Biol. Chem.* 251, 3359–3366.
16. Chakerian, A. E., and Matthews, K. S. (1991) *J. Biol. Chem.* 266, 22206–22214.
17. Chang, W.-I., Olson, J. S., and Matthews, K. S. (1993) *J. Biol. Chem.* 268, 17613–17622.
18. Adler, K., Beyreuther, K., Fanning, E., Geisler, N., Gronenborn, B., Klemm, A., Müller-Hill, B., Pfahl, M., and Schmitz, A. (1972) *Nature* 237, 322–327.
19. Kania, J., and Müller-Hill, B. (1977) *Eur. J. Biochem.* 79, 381–386.
20. Chen, J., and Matthews, K. S. (1994) *Biochemistry* 33, 8728–8735.
21. Chen J., Alberti, S., and Matthews, K. S. (1994) *J. Biol. Chem.* 269, 12482–12487.
22. Gilbert, W., and Müller-Hill, B. (1967) *Proc. Natl. Acad. Sci. U.S.A.* 58, 2415–2421.
23. Riggs, A. D., Bourgeois, S., Newby, R. F., and Cohn, M. (1968) *J. Mol. Biol.* 34, 365–368.
24. Riggs, A. D., Newby, R. F., and Bourgeois, S. (1970) *J. Mol. Biol.* 51, 303–314.
25. Barkley, M. D., Riggs, A. D., Jobe, A., and Bourgeois, S. (1975) *Biochemistry* 14, 1700–1712.
26. Lin, S.-Y., and Riggs, A. D. (1975) *Cell* 4, 107–111.
27. O’Gorman, R. B., Rosenberg, J. M., Kallai, O. B., Dickerson, R. E., Itakura, K., Riggs, A. D., and Matthews, K. S. (1980) *J. Biol. Chem.* 255, 10107–10114.
28. Daly, T. J., and Matthews, K. S. (1986) *Biochemistry* 25, 5479–5484.
29. Schumacher, M. A., Choi, K. Y., Zalkin, H., and Brennan, R. G. (1994) *Science* 266, 763–770.
30. Schumacher, M. A., Choi, K. Y., Lu, F., Zalkin, H., and Brennan, R. G. (1995) *Cell* 83, 147–155.
31. Yang, D. S., Burgum, A. A., and Matthews, K. S. (1977) *Biochim. Biophys. Acta* 493, 24–36.
32. Burgum, A. A., and Matthews, K. S. (1978) *J. Biol. Chem.* 253, 4279–4286.
33. Hsieh, W.-T., and Matthews, K. S. (1981) *J. Biol. Chem.* 256, 4856–4862.
34. Whitson, P. A., Burgum, A. A., and Matthews, K. S. (1984) *Biochemistry* 23, 6046–6052.
35. Ohshima, Y., Matsuura, M., and Horiuchi, T. (1972) *Biochem. Biophys. Res. Commun.* 47, 1444–1450.
36. Matthews, K. S., Matthews, H. R., Thielmann, H. W., and Jardetzky, O. (1973) *Biochim. Biophys. Acta* 295, 159–165.
37. Sams, C. F., Friedman, B. E., Burgum, A. A., Yang, D. S., and Matthews, K. S. (1977) *J. Biol. Chem.* 252, 3153–3159.
38. Brown, R. D., and Matthews, K. S. (1979) *J. Biol. Chem.* 254, 5135–5143.
39. Laiken, S. L., Gross, C. A., and von Hippel, P. H. (1972) *J. Mol. Biol.* 66, 143–155.
40. Sommer, H., Lu, P., and Miller, J. H. (1976) *J. Biol. Chem.* 251, 3774–3779.
41. Bandyopadhyay, P. K., and Wu, C.-W. (1979) *Arch. Biochem. Biophys.* 195, 558–564.
42. Gardner, J. A., and Matthews, K. S. (1990) *J. Biol. Chem.* 265, 21061–21067.
43. Wu, F. Y.-H., Bandyopadhyay, P., and Wu, C.-W. (1976) *J. Mol. Biol.* 100, 459–472.
44. Brown, M. P., Shaikh, N., Brenowitz, M., and Brand, L. (1994) *J. Biol. Chem.* 269, 12600–12605.
45. Weitzman, C., Consler, T. G., and Kaback, H. R. (1995) *Protein Sci.* 4, 2310–2318.
46. Watanabe, F., Jameson, D. M., and Uyeda, K. (1996) *Protein Sci.* 5, 904–913.
47. Cheung, C.-W., and Mas, M. T. (1996) *Protein Sci.* 5, 1144–1149.
48. Stole, E., and Bryant, F. R. (1994) *J. Biol. Chem.* 269, 7919–7925.
49. Nichols, J. C., Vyas, N. K., Quiocho, F. A., and Matthews, K. S. (1993) *J. Biol. Chem.* 268, 17602–17612.
50. Kunkel, T. A. (1985) *Proc. Natl. Acad. Sci. U.S.A.* 82, 488–492.
51. Li, L., and Matthews, K. S. (1995) *J. Biol. Chem.* 270, 10640–10649.
52. Bradford, M. M. (1976) *Anal. Biochem.* 72, 248–254.
53. Wong, I., and Lohman, T. M. (1993) *Proc. Natl. Acad. Sci. U.S.A.* 90, 5428–5432.
54. Bourgeois, S. (1971) *Methods Enzymol.* 21, 491–500.
55. Beechem, J. M., Gratton, E., Ameloot, M., Knutson, J. R., and Brand, L. (1989) in *Fluorescence Spectroscopy: Principles and Techniques* (Lakowicz, J. R., Ed.) Vol. 2, pp 241–306, Plenum Press, New York.
56. Chang, W.-I., and Matthews, K. S. (1995) *Biochemistry* 34, 9227–9234.
57. Lehrer, S. S. (1971) *Biochemistry* 10, 3254–3263.
58. Eftink, M. R., and Ghiron, C. A. (1976) *Biochemistry* 15, 672–679.
59. Friedman, B. E., Olson, J. S., and Matthews, K. S. (1977) *J. Mol. Biol.* 111, 27–39.
60. Brochon, J. C., Wahl, P., Charlier, M., Maurizot, J. C., and Hélène, C. (1977) *Biochem. Biophys. Res. Commun.* 79, 1261–1271.
61. Royer, C. A., Gardner, J. A., Beechem, J. M., Brochon, J.-C., and Matthews, K. S. (1990) *Biophys. J.* 58, 363–378.
62. Eftink, M. R., and Ghiron, C. A. (1981) *Anal. Biochem.* 114, 199–227.
63. Matthews, K. S. (1974) *Biochim. Biophys. Acta* 359, 334–340.
64. Boschelli, F., Jarema, M. A. C., and Lu, P. (1981) *J. Biol. Chem.* 256, 11595–11599.
65. Jarema, M. A. C., Lu, P., and Miller, J. H. (1981) *Proc. Natl. Acad. Sci. U.S.A.* 78, 2707–2711.
66. O’Gorman, R. B., and Matthews, K. S. (1977) *J. Biol. Chem.* 252, 3565–3571.
67. O’Gorman, R. B., and Matthews, K. S. (1977) *J. Biol. Chem.* 252, 3572–3577.
68. Kelsey, D. E., Rounds T. C., and York, S. S. (1979) *Proc. Natl. Acad. Sci. U.S.A.* 76, 2649–2653.
69. Suckow, J., Markiewicz, P., Kleina, L. G., Miller, J., Kisters-Woike, B., and Müller-Hill, B. (1996) *J. Mol. Biol.* 261, 509–523.
70. Chuprina, V. P., Rullmann, J. A. C., Lamerichs, R. M. J. N., van Boom, J. H., Boelens, R., and Kaptein, R. (1993) *J. Mol. Biol.* 234, 446–462.
71. Carson, M. (1987) *J. Mol. Graphics* 5, 103–106.

BI971685R